

into an integrated percept<sup>17</sup>, and it is these integrated object percepts that appear to be stored in visual working memory. Neurobiological accounts of working memory must therefore include a mechanism for keeping the features of an object bound together during the retention interval. A leading candidate mechanism is the use of oscillatory or temporally correlated firing patterns among the neurons that code the features of an object<sup>18–20</sup>. Such a mechanism can also readily explain the relatively small number of objects that can be held in working memory concurrently: as the number of concurrent objects increases, the possibility of accidental correlations between neurons that code different objects also increases<sup>7</sup>. However, this would not necessarily place any limits on the number of features that can be bound together into a single object representation, which is consistent with our findings. □

**Methods**

Ten neurologically normal college students participated in each experiment. Each of these observers received 32–40 trials in each condition, where a condition consisted of a combination of set size and some other variable, such as the presence or absence of a verbal load.

All stimulus arrays were presented within a 9.8° × 7.3° region on a video monitor with a grey background (8.2 cd m<sup>-2</sup>), and the items in a given array were separated by at least 2.0° (centre to centre). One feature of one item in the test array was different from the corresponding item in the sample array on 50% of trials; the sample and test arrays were otherwise identical.

The experiments shown in Fig. 1a used sample arrays consisting of 1, 2, 3, 4, 8 or 12 coloured squares (0.65° × 0.65°), each of which was selected at random from a set of 7 highly discriminable colours (red, blue, violet, green, yellow, black and white). The experiments shown in Fig. 1b used the same stimuli, but set size was limited to 4, 8 or 12 items.

The experiments testing combinations of colour and orientation (Fig. 1c) used arrays of 0.03° × 1.15° rectangles, each of which was constructed by combining one of four orientations (vertical, horizontal, -45° and +45°) with one of four colours (red, green, blue and black). The stimuli used in the experiment shown in Fig. 1d were combinations of horizontal or vertical, red or green, small or large (0.13° × 1.0° or 0.13° × 2.0°) and continuous or broken (broken by a 0.26° black gap).

The colour–colour conjunction stimuli shown in Fig. 1e consisted of a small square (0.65° × 0.65°) embedded in a large square (1.3° × 1.3°). The inner and outer colours for a given object were selected from the set of red, green, violet and blue with the constraint that the inner and outer colours were always different from each other. The simple feature conditions of this experiment used either the large squares presented alone or the small squares presented alone.

Received 16 June; accepted 20 August 1997.

1. Baddeley, A. D. *Working Memory* (Clarendon, Oxford, 1986).
2. Jonides, J. et al. Spatial working memory in humans as revealed by PET. *Nature* **363**, 623–625 (1993).
3. Miller, E. K., Erickson, C. A. & Desimone, R. Neural mechanisms of visual working memory in prefrontal cortex of the macaque. *J. Neurosci.* **16**, 5154–5167 (1996).
4. Wilson, F. A. W., O'Scalaidhe, S. P. & Goldman-Rakic, P. S. Dissociation of object and spatial processing domains in primate prefrontal cortex. *Science* **260**, 1955–1958 (1993).
5. Paulesu, E., Frith, C. G. & Frackowiak, R. S. J. The neural correlates of the verbal component of working memory. *Nature* **362**, 342–345 (1993).
6. Fuster, J. M. *Memory in the Cerebral Cortex: An Empirical Approach to Neural Networks in the Human and Nonhuman Primate* (MIT Press, Cambridge, MA, 1995).
7. Lisman, J. E. & Idiart, M. A. P. Storage of 7+/-2 short-term memories in oscillatory subcycles. *Science* **267**, 1512–1515 (1995).
8. Phillips, W. A. On the distinction between sensory storage and short-term visual memory. *Percept. Psychophys.* **16**, 283–290 (1974).
9. Pahlner, H. Familiarity and visual change detection. *Percept. Psychophys.* **44**, 369–378 (1988).
10. Palmer, J. Attentional limits on the perception and memory of visual information. *J. Exp. Psychol. Hum. Percept. Perform.* **16**, 332–350 (1990).
11. Green, D. M. Detection of auditory sinusoids of uncertain frequency. *J. Acoust. Soc. Am.* **33**, 897–903 (1961).
12. Palmer, J. Set-size effects in visual search: the effect of attention is independent of the stimulus for simple tasks. *Vision Res.* **34**, 1703–1721 (1994).
13. Palmer, J., Ames, C. T. & Lindsey, D. T. Measuring the effect of attention on simple visual search. *J. Exp. Psychol. Hum. Percept. Perform.* **19**, 108–130 (1993).
14. Cohen, A. & Ivry, R. Illusory conjunctions inside and outside the focus of attention. *J. Exp. Psychol. Hum. Percept. Perform.* **15**, 650–663 (1989).
15. Miller, G. A. The magical number seven, plus or minus two: Some limits on our capacity for processing information. *Psychol. Rev.* **63**, 81–97 (1956).
16. Duncan, J. Selective attention and the organization of visual information. *J. Exp. Psychol. Gen.* **113**, 501–517 (1984).
17. Treisman, A. The binding problem. *Curr. Opin. Neurobiol.* **6**, 171–178 (1996).

18. Singer, W. & Gray, C. M. Visual feature integration and the temporal correlation hypothesis. *Annu. Rev. Neurosci.* **18**, 555–586 (1995).
19. Niebur, E., Koch, C. & Rosin, C. An oscillation-based model for the neuronal basis of attention. *Vision Res.* **33**, 2789–2802 (1993).
20. Luck, S. J. & Beach, N. J. in *Visual Attention* (ed. Wright, R.) (Oxford Univ. Press, in the press).
21. Sperling, G. The information available in brief visual presentations. *Psychol. Monogr.* **74** (1960).

**Acknowledgements.** This research was supported by grants from the McDonnell-Pew Program in Cognitive Neuroscience and the National Institute of Mental Health.

Correspondence and requests for materials should be addressed to S.J.L. (steven-luck@uiowa.edu).

## A role for the Ras signalling pathway in synaptic transmission and long-term memory

Riccardo Brambilla\*†‡, Nerina Gnesutta\*§, Liliana Minichiello†, Gail White||, Alistair J. Roylance¶, Caroline E. Herron¶#, Mark Ramsey#, David P. Wolfer\*, Vincenzo Cestari\*\*, Clelia Rossi-Arnaud††, Seth G. N. Grant†#, Paul F. Chapman||, Hans-Peter Lipp\*, Emmapaola Sturani§ & Rüdiger Klein†

† European Molecular Biology Laboratory, Meyerhofstrasse 1, 69117 Heidelberg, Germany

§ Dipartimento di Fisiologia e Biochimica Generali, Università di Milano, 20133 Milano, Italy

|| Physiology Unit, School of Molecular and Medical Biosciences, University of Wales, Cardiff CF1 3US, UK

¶ Centre for Genome Research, University of Edinburgh, Edinburgh EH9 3JQ, UK

# Centre for Neuroscience, University of Edinburgh, Edinburgh EH8 9LE, UK

\* Anatomisches Institut, Universität Zürich, CH-8057 Zürich, Switzerland

\*\* Istituto di Psicobiologia e Psicofarmacologia del Consiglio Nazionale delle Ricerche, 00198 Roma, Italy

†† Dipartimento di Psicologia, Università di Roma 'La Sapienza', 00185 Roma, Italy

\* These authors contributed equally to this work.

Members of the Ras subfamily of small guanine-nucleotide-binding proteins are essential for controlling normal and malignant cell proliferation as well as cell differentiation<sup>1</sup>. The neuronal-specific guanine-nucleotide-exchange factor, Ras-GRF/CDC25Mm (refs 2–4), induces Ras signalling in response to Ca<sup>2+</sup> influx<sup>5</sup> and activation of G-protein-coupled receptors *in vitro*<sup>6</sup>, suggesting that it plays a role in neurotransmission and plasticity *in vivo*<sup>7</sup>. Here we report that mice lacking Ras-GRF are impaired in the process of memory consolidation, as revealed by emotional conditioning tasks that require the function of the amygdala; learning and short-term memory are intact. Electrophysiological measurements in the basolateral amygdala reveal that long-term plasticity is abnormal in mutant mice. In contrast, Ras-GRF mutants do not reveal major deficits in spatial learning tasks such as the Morris water maze, a test that requires hippocampal function. Consistent with apparently normal hippocampal functions, Ras-GRF mutants show normal NMDA (N-methyl-D-aspartate) receptor-dependent long-term potentiation in this structure. These results implicate Ras-GRF signalling via the Ras/MAP kinase pathway in synaptic events leading to formation of long-term memories.

Several distinct mechanisms leading to Ras activation and initiation of the MAP kinase (MAPK) cascade have been elucidated<sup>8</sup>. Growth-factor receptors of the tyrosine kinase family activate Ras proteins by recruiting the ubiquitously expressed Sos exchange

‡ Present address: DIBIT, Istituto Scientifico San Raffaele, Via Olgettina 58, 20132 Milano, Italy.

factors to the cell membrane through the adapter protein Grb2 (ref. 9). In neurons, an increase in intracellular calcium levels activates the Ras/MAPK pathway<sup>10</sup>.

The exchange factor Ras-GRF (also called CDC25Mm) is exclusively expressed in neurons of the postnatal and adult central nervous system (CNS)<sup>11</sup> and is mainly localized in the synaptosomal fraction<sup>12</sup>. Following activation of muscarinic M1 and M2 receptors, Ras-GRF becomes phosphorylated and this increases its exchange activity<sup>6</sup>. Instead of presenting a Grb2-binding domain, Ras-GRF contains an ilimaquinone domain. When intracellular calcium is increased, this domain is necessary for binding to Ca<sup>2+</sup>-calmodulin and for Ras-GRF-dependent activation of the Ras/MAPK pathway<sup>5</sup>.

To examine the role of Ras-GRF in the activity of the adult brain, we inactivated the mouse gene using homologous recombination in embryonic stem (ES) cells, by replacing the most 5' region encoding the exchange-factor catalytic domain with the phosphoglycerate kinase (PGK) promoter-driven neomycin cassette (Fig. 1a). Ras-GRF<sup>-/-</sup> mice are viable and fertile. To characterize the mutant mice at the molecular level, we generated amino-terminal-specific antibodies against Ras-GRF. Using NIH3T3 cells expressing full-length Ras-GRF in immunoprecipitation assays, we showed that commercially available anti-C-terminal and our anti-N-terminal antiserum specifically recognized a single band of relative molecular mass (*M<sub>r</sub>*) 140K, corresponding to the Ras-GRF gene product (Fig. 1b). Detection of p140 was competent with the corresponding antigen, the PHP fragment of Ras-GRF, further demonstrating the specificity of the N-terminal antibodies. We performed western blot analysis on brain extracts using the two different antisera. The N-terminal antibodies specifically and exclusively recognized p140<sup>Ras-GRF</sup> only in mice carrying the wild-type allele, demonstrating that the introduced mutation resulted in the complete loss of the p140<sup>Ras-GRF</sup> gene product (Fig. 1c). The same loss of signal was also demonstrated using the C-terminal-specific antibodies.

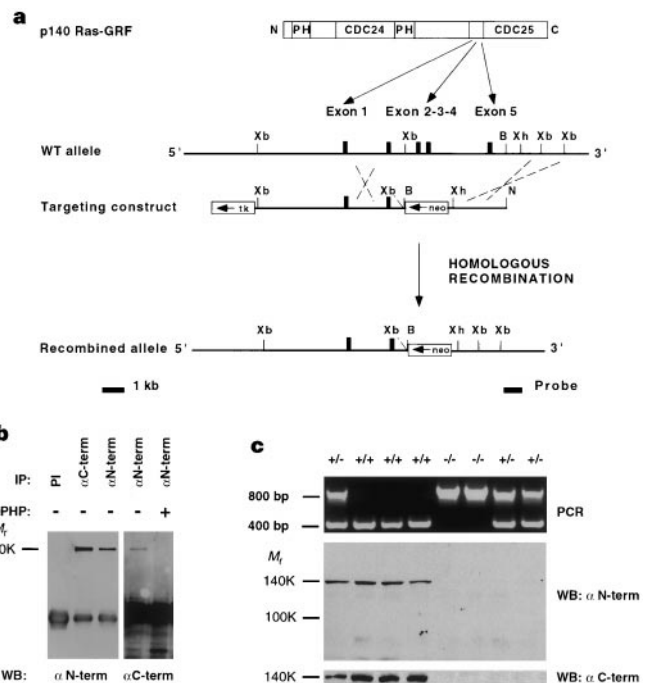
Interestingly, some of the Ras-GRF<sup>+/-</sup> mice also lacked p140<sup>Ras-GRF</sup> and by western blot analysis were indistinguishable from Ras-GRF<sup>-/-</sup> mice (Fig. 1c). A new imprinted locus on mouse chromosome 9, corresponding to that of Ras-GRF, has been identified<sup>13</sup>. Our data on Ras-GRF heterozygotes confirmed the reported paternal allele-specific expression (data not shown).

The biological significance of this phenomenon, however, is unknown.

Histological analysis was carried out on adult brains of wild-type and Ras-GRF mutant mice. Nissl-stained coronal sections of mutant mice did not show morphological abnormalities (Fig. 2a, b), despite the fact that Ras-GRF is widely expressed in many CNS structures, including hippocampus, cerebral cortex and thalamus, as shown by *in situ* hybridization analysis of wild-type animals (Fig. 2c). No expression of Ras-GRF messenger RNA was detected in brain sections derived from Ras-GRF<sup>-/-</sup> mice (Fig. 2d). To study specific subpopulations of neurons in more detail, we used as markers the calcium-binding proteins calbindin-D28K, parvalbumin and calretinin, which are thought to have roles in buffering intracellular calcium and are expressed in different subgroups of neurons<sup>14</sup>. Staining patterns were identical in Ras-GRF<sup>-/-</sup> and wild-type mice, indicating that these calcium-binding proteins were expressed at normal levels (data not shown). Based on the observed behavioural phenotype (see below), we analysed the amygdala in more detail (Fig. 2e, f). This structure also contains high levels of Ras-GRF mRNA and has a normal appearance in the mutants, based on Nissl staining (not shown) and calbindin immunoreactivity. No signs of neuronal atrophy were detected at high magnification (Fig. 2f, inset). In conclusion, our histological analysis did not reveal any major morphological defects in Ras-GRF mutant mice.

Because Ras-GRF-dependent signalling may have a role in synaptic transmission and plasticity, Ras-GRF<sup>-/-</sup> mice were subjected to behavioural tests. The two-way avoidance test is a measure for both conditioned learning and emotional response to aversive (noxious) stimuli<sup>15</sup>. In this test, mice are placed in a two-chamber box and taught to avoid a signalled electric shock (unconditioned stimulus) by running into the opposite compartment. The shock is preceded by a warning light (conditioned stimulus). The role of the amygdala has been clearly demonstrated for this test, as for other emotional learning tests<sup>16</sup>. As shown in Fig. 3a, wild-type mice gradually learned to avoid the electric shock with a 40% success rate by day 5 of the experiment. The performance of Ras-GRF mutant mice was much worse, showing a less than 10% success rate on the same day (*P* < 0.0001). Dose-response curves using increasing shock

**Figure 1** Generation of a targeted mutation in the mouse Ras-GRF gene. **a**, protein structure, genomic structure and targeting strategy. Location of the 2 pleckstrin homology (PH) domains, the CDC24-like domain and CDC25-like domain are indicated on the structure of p140<sup>Ras-GRF</sup>. Five exons (designated 1-5) encoding amino-acid sequences N-terminal to the CDC25-like catalytic domain were mapped and sequenced in the murine wild-type Ras-GRF gene and are indicated as vertical bars. A 4-kb region of Ras-GRF containing exons 3-5 was replaced by the PGK promoter-driven neomycin cassette. This caused an increase of 2 kb of a diagnostic *Bam*HI fragment. Two different recombinant clones were used to generate mice carrying the Ras-GRF mutation which were subsequently used for the behavioural tests. Restriction sites: B, *Bam*HI; N, *Not*I; Xb, *Xba*I; Xh, *Xho*I. **b**, Characterization of new polyclonal antibodies against the N-terminal domain of Ras-GRF. Lysates of NIH3T3 cells ectopically expressing Ras-GRF were immunoprecipitated with preimmune serum (lane 1), anti Ras-GRF C-20 antibodies (Santa Cruz Biotech.) (lane 2), affinity-purified anti-N-terminal antibodies in the absence (lanes 3, 4) or presence of the purified PHP antigen (lane 5). After SDS-PAGE, blots were probed with affinity-purified N-terminal (lanes 1, 2, 3) or with C-20 (lanes 4, 5) antibodies. The specific 140K band is indicated. **c**, Biochemical analysis of Ras-GRF mutant mice. A litter of 1-month-old animals derived from a cross between two heterozygotes was first genotyped using polymerase chain reaction (PCR): 400 bp DNA fragment, wild-type allele; 800 bp DNA fragment, mutant allele. Brain extracts were prepared and subjected to western blot analysis with either anti-N-terminal or anti-C-terminal Ras-GRF-specific antisera. Positions of the 140K wild-type protein and of the 100K molecular marker are indicated.



intensities did not show differences between groups, ruling out a possible difference in shock sensitivity (data not shown). Other parameters such as pre-session activity were found to be normal ( $P > 0.5$ ), indicating that the motor activity of both groups in the absence of conditioned stimulus was comparable (not shown). In addition, we have also tested a second Ras-GRF line derived from an independent ES clone targeted in the same way as above. This mutant strain also gave statistically significant impairment in avoidance learning (data not shown).

The one-trial inhibitory avoidance test makes use of the natural tendency of mice to move from an illuminated into a dark compartment<sup>17</sup>. Once the animal is in the dark compartment, it receives an electric shock. One single trial is normally sufficient for learning the task, which is to avoid the dark compartment during the probing trial (0.5 h to measure learning and short-term memory or 24 h to measure long-term memory). Note that this test requires no motor activity to manifest learning, in contrast to the two-way avoidance test. Both wild-type and Ras-GRF mutants clearly learn to avoid the dark compartment (Fig. 3b). The step-through latency time at 0.5 h increased in comparison to untrained mice ( $P < 0.0001$ ), but no differences were detected between the groups ( $P > 0.1$ ). In contrast, at 24 h, although wild-type mice persistently avoided the dark chamber, mutant mice seemed to have largely forgotten the task because they ran into the compartment with a latency intermediate between that of 0.5 h and untrained mice ( $P < 0.0001$  between the two groups, at 24 h).

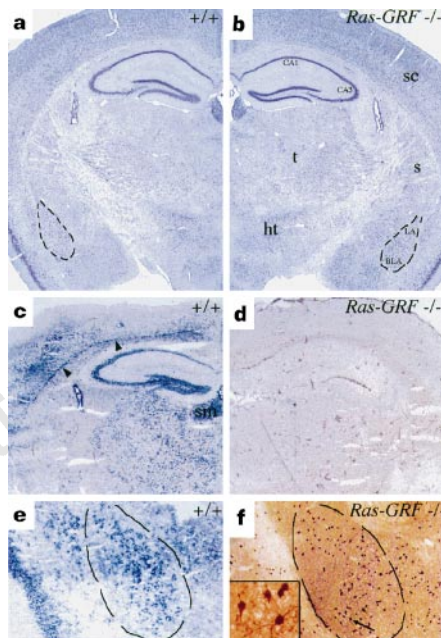


**Figure 2** Ras-GRF mutant mice do not show gross morphological abnormalities in the brain. **a, b**, Coronal sections of wild-type and Ras-GRF mutant adult brains, stained with cresyl violet (Nissl). Note the normal appearance of the brain structures. sc, Somatosensory cortex; t, thalamus; s, striatum; ht, hypothalamus; LA, lateral nucleus of the amygdala; BLA, basolateral nucleus of the amygdala (stippled line). **c**, expression pattern of Ras-GRF mRNA by *in situ* hybridization. Note high expression levels in hippocampal structures and in the stria medullaris (sm), wide expression in the thalamus and in different cortical layers with more intense staining in a subpopulation of neurons located in layer VI (arrowheads). **d**, No expression of Ras-GRF was detected in the mutant section corresponding to **c**. **e**, Expression of Ras-GRF mRNA in the wild-type amygdala. **f**, Normal appearance of the lateral and basolateral nuclei of the amygdala of Ras-GRF mutant mice stained with calbindin-D28K. Inset in **f** is a higher magnification (neurons indicated with an arrow). Magnification: **a-d**, X25; **e, f**, X200; inset, X1,000.

One-session fear conditioning can also be studied using a technique in which the foot shock used as an unconditioned stimulus is of higher intensity than in the shuttle-box, but only applied during a short period. When exposed to conditioned stimulus again, conditioned animals show an immobility ('freezing') reaction during which the animals refrain from all but respiratory movements. Freezing responses can be triggered with two different types of conditioned stimulus, each involving different brain structures<sup>18</sup>. In contextual conditioning, the conditioned stimulus is represented by the environment in which the unconditioned stimulus is delivered. This type of conditioning appears to depend on both hippocampal and amygdalar functions. In cued conditioning, the conditioned stimulus is a tone, and this type of conditioning is disrupted by lesions of the amygdala but not of the hippocampus. Mice were conditioned to tone and context during the same trial session and then tested separately, 0.5 and 24 h later. For measuring contextual learning, mice were placed in the same box where the training occurred and freezing was monitored for 2 min (Fig. 3c). At 0.5 h after conditioning, both wild-type and mutant mice showed the same freezing response, without significant difference ( $P > 0.1$ ) but statistically higher than untrained mice ( $P < 0.0001$ ). However, at 24 h, although wild-type mice still retained a strong freezing response, Ras-GRF mutants showed a dramatically reduced response ( $P < 0.0001$ ). For measuring cued conditioning, mice were placed in a neutral cage for 1 min to minimize the contextual response, before delivering a continuous

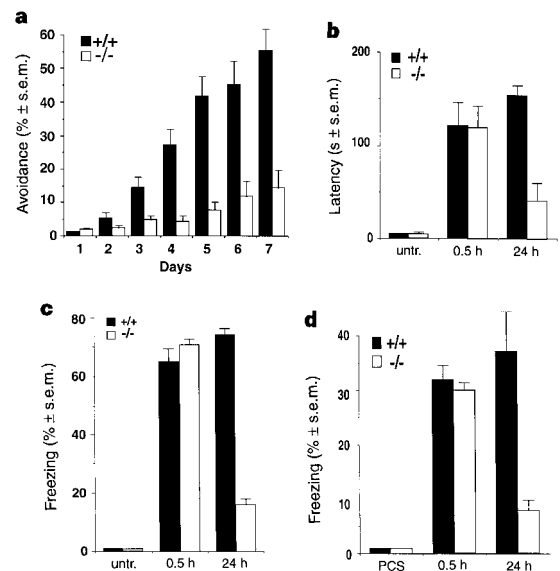


**Figure 3** Impaired memory consolidation in Ras-GRF mutant mice during fear conditioning tests. **a**, Two-way avoidance learning test. Mice (wild-type,  $n = 24$ ; mutants,  $n = 26$ ) were trained for 7 days, 80 trials a day. Percentage of correct responses (avoidance of the shock) is shown. **b**, One-trial inhibitory avoidance test. Different groups of mice were tested for step-through latencies into the dark compartment: untr., untrained mice (wild-type  $n = 18$ ; mutant  $n = 18$ ), 0.5 h (wild-type  $n = 8$ ; mutant  $n = 8$ ) or 24 h (wild-type  $n = 10$ ; mutant  $n = 10$ ) after training. Mean step-through latencies expressed in  $s \pm s.e.m.$  are indicated for both groups. **c**, Contextual fear conditioning test. Wild-type ( $n = 12$ ) and mutant mice ( $n = 10$ ) were tested before training (untr.), 0.5 h and 24 h after training for freezing (2 min) in the same training box. **d**, Cued fear conditioning test. The same mice used for contextual conditioning were subsequently tested 0.5 h and 24 h after training for freezing in the presence of a sound continuous for 1 min in a neutral cage, different from the training box, to minimize context-dependent freezing response. PCS is the pre-conditioned stimulus phase of 1 min. Cumulative percentages of freezing  $\pm s.e.m.$  are indicated.

tone for 1 min (Fig. 3d). As observed for the one-trial inhibitory avoidance test and contextual fear conditioning, acquisition and short retention of the task appeared normal in the Ras-GRF<sup>-/-</sup> mice, whereas long-term memory was significantly diminished ( $P < 0.0001$ ).

In conclusion, all these emotional learning paradigms clearly demonstrate that Ras-GRF<sup>-/-</sup> mice are severely impaired at the level of memory consolidation, rather than in the learning process itself.

In contrast to amygdala-mediated fear conditioning, spatial learning mainly depends on the function of the hippocampus<sup>19</sup>. To monitor spatial learning in rodents, animals were subjected to the Morris swimming navigation test<sup>20</sup>. In this test, the animal is placed in a pool and learns to find a submerged platform using visual cues outside the maze. After the intensive acquisition phase lasting 3 days, the platform is moved to the opposite position to test first for spatial learning of the former position (first trial, day 4) and subsequently for suppression of the old spatial information and

reprogramming towards the new goal position (day 4 and 5). Clear learning curves were observed for the mutants ( $P < 0.001$ ), with no differences in escape latency between mutant and control mice ( $P > 0.1$ ) (Fig. 4a). Further evidence for normal spatial learning in both groups came from the retention test (Fig. 4b). During the first trial after the platform was moved to the opposite position, both groups showed preferential searching in the old goal quadrant relative to the others ( $P < 0.0001$ ) but no differences between genotypes were seen ( $P > 0.1$ ), indicated as the number of annulus quadrant crossings.

The radial-arm maze is another sensitive assay for hippocampal function. The advantage over the swimming test is that much less demanding motor activity is required to perform the task and different strategies can be used by the animal to explore the environment. Animals with hippocampal lesions are clearly impaired when tested on this task<sup>21</sup>. The performance of wild-type and mutant Ras-GRF mice was compared in a radial 8-arm maze with cues outside the maze. The procedure used allows the animals to visit each arm, searching for the food reward at any time. Variance analysis on the number of correct arm choices demonstrated that both groups of mice made significant progress in learning performance on the radial maze over the ten training sessions ( $P < 0.0001$ ) (Fig. 4c). Both groups reached roughly the same level of performance and no difference between groups was apparent ( $P > 0.1$ ). In addition, no differences in the strategy used to explore the arm were seen between the two groups (not shown). These data indicate that Ras-GRF mutants do not show major deficits in standard tests of hippocampal function.

To analyse several aspects of synaptic physiology and plasticity we performed electrophysiological experiments in the CA1 region of hippocampus and in the basolateral amygdala. In particular, we tested long-term potentiation (LTP), which is believed to be an important physiological event underlying learning and memory formation<sup>22</sup>. In CA1, stimulation of the Schaffer collateral pathway at 100 Hz in slices from Ras-GRF mutant and wild-type mice induced LTP of the synaptic response (Fig. 5a). This potentiation was not significantly different in slices from mutant mice ( $162 \pm 14\%$ ;  $n = 11$  slices, 5 animals) compared to slices from wild-type mice ( $158 \pm 13.8\%$ ;  $n = 13$  slices, 6 animals). The induction of LTP under these conditions was blocked when tetani were delivered in the presence of the NMDA receptor antagonist D-AP5 ( $50 \mu\text{M}$ ) (data not shown). Extracellular field potential responses were recorded in the basolateral amygdala, which is known to support plasticity *in vitro*<sup>23</sup>. Delivery of 3 trains of stimulation of 10-burst theta frequency stimulation produced significant LTP (Fig. 5b, c) in  $+/+$  controls ( $134 \pm 12\%$  of baseline;  $n = 8$  mice, 16 slices), whereas  $-/-$  mice showed no such enhancement ( $104 \pm 3\%$  of baseline;  $n = 7$  mice, 11 slices,  $P < 0.001$ ). Although long-lasting plasticity was absent in  $-/-$  mice, there were no differences ( $P = 0.78$ ) between the two groups in the first minute after tetanus ( $-/-$ ,  $122 \pm 3\%$ ;  $+/+$ ,  $124 \pm 4\%$ ). When theta-burst tetanus was delivered to Schaffer collaterals in the CA1 region of hippocampal slices (taken from the same mice as the amygdala slices) LTP in  $-/-$  mice ( $130 \pm 13\%$  of baseline,  $n = 6$  mice) was not different from LTP in  $+/+$  mice ( $121 \pm 10\%$  of baseline,  $n = 4$  mice,  $P > 0.5$ , Fig. 5b). Analysis of baseline synaptic response properties revealed that Ras-GRF<sup>-/-</sup> mice showed larger field excitatory post-synaptic potentials (EPSPs) in amygdala than  $+/+$  mice (mean across intensities for  $-/-$  mice was  $0.94 \pm 0.04 \text{ V s}^{-1}$ ;  $n = 9$  mice, 15 slices; for  $+/+$  mice,  $0.54 \pm 0.04$ ,  $n = 14$  mice, 25 slices) and in CA1 of hippocampus (mean across intensities for  $-/-$  mice was  $2.55 \pm 0.14 \text{ V s}^{-1}$ ;  $n = 8$  mice, 10 slices; for  $+/+$  mice,  $1.44 \pm 0.12$ ;  $n = 11$  mice, 14 slices), across a range of stimulus intensities (Fig. 5e). Analysis of variance indicates that the differences were significant in both structures ( $P < 0.0001$ ). In the hippocampus, it is possible to use the amplitude of the presynaptic fibre volley to estimate the strength of afferent inputs, and thus

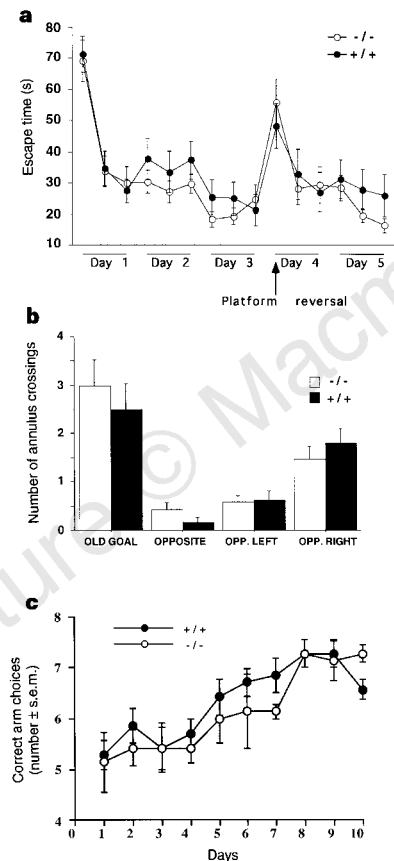


**Figure 4** Hippocampal-dependent behaviour appears to be normal in Ras-GRF mutant mice. **a**, Spatial learning test. Wild-type ( $n = 24$ ) and mutant mice ( $n = 24$ ) were trained for 3 consecutive days (6 trials per day) with the submerged platform (acquisition phase) which was followed by 2 days of reversal phase, with the platform at the opposite position in the pool. Escape latency is expressed in seconds required to find the platform. **b**, Number of annulus crossings of the quadrants at the probing trial (day 4, trial 1). The value is indicated for all four quadrants: old goal, old training quadrant; opposite, opposite quadrant to the old goal position; opp. left, adjacent left quadrant to the old goal; opp. right, adjacent right quadrant to the old goal. **c**, Radial-maze test. Wild-type ( $n = 14$ ) and mutant ( $n = 14$ ) mice were trained for 10 consecutive days in an eight-arm radial maze. Learning performance is expressed in terms of the mean number of correct arm choices on each trial. The number observed at day 1 was taken as the starting point ( $5.28 \pm 0.28$  for wild-type;  $5.14 \pm 0.59$  for mutants).

compare the synaptic input/output values more directly. Measurements of the ratio of the EPSP slope to the fibre volley amplitude (Fig. 5f) also indicated significant differences ( $P < 0.0001$ ) between  $+/+$  mice (mean ratio =  $2.27 \pm 0.23$ ;  $n = 11$  mice, 13 slices) and Ras-GRF $-/-$  mice (mean ratio =  $3.96 \pm 0.27$ ;  $n = 8$  mice, 10 slices). Finally, we examined paired-pulse facilitation (Fig. 5d), a form of short-lasting plasticity that depends on presynaptic mechanisms<sup>24</sup>. In hippocampus, wild-type mice show paired-pulse facilitation values ( $1.38 \pm 0.07$ ) that were statistically indistinguishable from Ras-GRF mutant slices ( $1.30 \pm 0.02$ ,  $P > 0.5$ ). The same was observed for amygdala slices (for  $+/+$ ,  $1.27 \pm 0.05$ ; for  $-/-$ ,  $1.19 \pm 0.03$ ,  $P > 0.1$ ), suggesting that Ras-GRF is not absolutely necessary for this type of plasticity.

We have shown that Ras-GRF mutant mice have an impairment in the process of memory consolidation during fear-related behavioural tasks and electrophysiological impairments in the amygdala, a critical part of the neural circuitry involved in emotional responses. The role of the amygdala in regulation of the behavioural response to external and noxious stimuli has been clearly demonstrated<sup>25,26</sup>. In rats, lesions in the amygdala dramatically affect acquisition of both cued and contextual fear conditioning, whereas specific lesions at the level of the hippocampus affect only contextual fear conditioning<sup>18</sup>. In contrast, Ras-GRF mutant mice do not show deficits in the learning process itself, implying that Ras-GRF signalling seems to be specifically involved in the consolidation of long-term memory.

Although Ras-GRF is highly expressed in the CA1 region of the rodent hippocampus, we did not detect, using several standard protocols, any major abnormalities in hippocampal synaptic plasticity or hippocampus-dependent forms of learning. We cannot infer that hippocampal functions are completely normal, as there are differences in some aspects of synaptic transmission, and there may be changes in other forms of plasticity. In any case, Ras-GRF does not seem absolutely required for spatial learning. Alternatively, some compensatory events might have occurred in the Ras-GRF mutants to mask the hippocampal phenotype.

Currently there is little information on the mechanisms by which Ras-GRF might be involved in processes leading to changes in synaptic transmission and LTP. We favour the idea that Ras-GRF signalling is directly involved in synaptic plasticity, although an indirect effect on the activity of certain types of neurons in the amygdala cannot formally be excluded. The differential effects on synaptic plasticity between amygdala and hippocampus may reflect the ability of Ras-GRF to couple with distinct signal transduction mechanisms that predominate in each of these structures. LTP in the CA1 region of the hippocampus requires calcium influx via the NMDA receptor, in contrast to at least some important pathways in the basolateral amygdala in which LTP is NMDA receptor-independent<sup>27</sup>. Moreover, muscarinic receptors are highly expressed in the basolateral amygdala and muscarinic antagonists block LTP in this structure<sup>28</sup>. Because muscarinic receptors activate Ras-GRF, producing an increase in its phosphorylation<sup>6</sup>, this pathway may be physiologically relevant to amygdala function. Thus Ras-GRF may be important in synapses where metabotropic receptors dominate synaptic plasticity and less important in those regulated by NMDA receptors.

Knockout experiments have demonstrated a role in long-term plasticity and behaviour for a number of protein kinase cascades<sup>29</sup>. Our finding that the Ras/Raf/MAP kinases pathway controlled by Ras-GRF is also involved in such processes strengthens the notion that multiple signalling events are simultaneously required for the generation of long-lasting synaptic changes, leading to consolidation of learning and memory processes. □

Methods

**Generation of targeted mice.** To construct the Ras-GRF targeting vector, a 1.3 kb *XhoI*-*NotI* and 5.6 kb *XbaI*-*XbaI* DNA fragments of cloned 129 strain Ras-GRF genomic DNA were used. After homologous recombination, a neomycin-resistance cassette was inserted while deleting 4 kb of the Ras-GRF locus, including exons 3–5 coding for the 5' portion of the CDC25-like catalytic domain (nucleotides 2,982–3,260 of the published cDNA sequence)<sup>3</sup>. Germline-transmitting chimaeras from two recombinant cell lines were

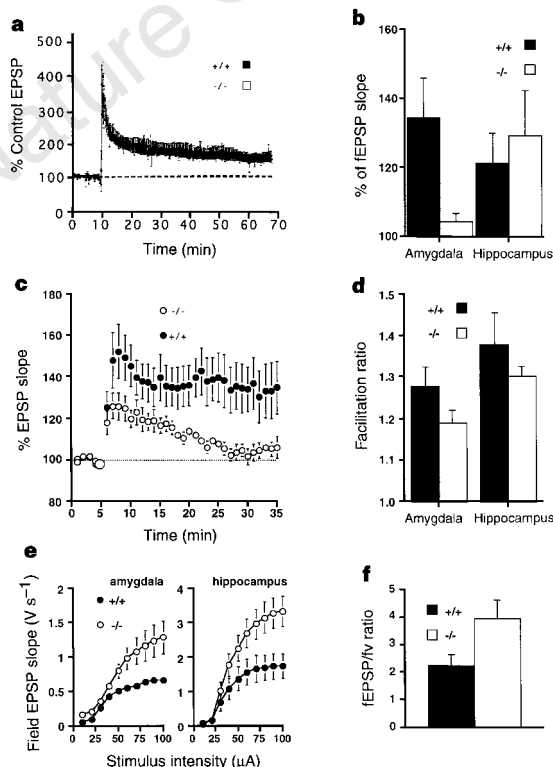


**Figure 5** Impaired synaptic plasticity in the amygdala of Ras-GRF $-/-$  mice. **a**, LTP in the hippocampus is unaffected by the Ras-GRF mutation following 2 trains of 100 stimuli each at 100 Hz. **b**, In both control and mutant hippocampal slices, theta-burst stimulation produces significant potentiation. **b, c** In  $+/+$  amygdala slices, theta-burst stimulation is also an extremely effective protocol for LTP induction, but amygdala slices taken from  $-/-$  mice do not demonstrate significant potentiation 30 min after tetanus. **d**, Paired pulse facilitation is not different between wild-type and Ras-GRF $-/-$  mice, in either the hippocampus or the amygdala. The indicated data are the average across the 30–100  $\mu$ A range of stimulus intensities, at 30-ms interpulse intervals. **e**, Synaptic responses are significantly elevated in both amygdala slices (left) and hippocampal slices (right) taken from Ras-GRF $-/-$  mice, compared to  $+/+$  controls. **f**, After controlling for variability in afferent input strength by measuring the ratio of the field EPSP slope to the fibre volley amplitude in hippocampal slices, the difference between  $+/+$  and  $-/-$  mice was still significant.

obtained by standard injection into C57BL/6 blastocysts, and the mutation was crossed into either 129/Sv or C57BL/6 genetic backgrounds.

**Biochemistry.** The Ras-GRF N-terminal fragment (PHP) corresponding to residues 1–149 of the published sequence<sup>3</sup> was used to raise specific antibodies. Total adult brain protein lysates were subjected to western blot analysis using polyclonal antibodies directed either against the N-terminal or the C-terminal portion of p140<sup>Ras-GRF</sup>. Blots were developed using the ECL method.

**Histology.** For immunohistochemistry, 40- $\mu$ m coronal cryosections were prepared and further processed using standard techniques. For *in situ* hybridization analysis, 16- $\mu$ m sections were prepared and processed following the manufacturer's protocol for digoxigenin-labelled oligonucleotide probes (Boehringer Mannheim). The DNA fragment used as a probe corresponds to 3' sequences of the published cDNA sequence of mouse Ras-GRF (nucleotides 1,915–4,174).

**Behavioural tests.** The mice used for all the behavioural tests were littermates of 9–16 weeks of age, kept on a 1:1 mixed genetic background between 129/Sv and C57BL/6. All the behavioural tests were performed as previously described<sup>15,17,20,21,30</sup>. In brief, for the two-way avoidance test, mice were placed in sound-proof shuttle-boxes (Campden Instruments) operated by a computer. After 2 min during which the mice were left undisturbed (pre-session), a conditioning light stimulus lasting 5 s was delivered and followed by a 10 s electric shock of 0.15 mA. Intertrial interval varied between 5 and 15 s. The animals underwent 80 trials a day for 7 days.

For the one-trial inhibitory avoidance test, mice were trained on an apparatus in which a straight alley was divided into two compartments. The smaller compartment was made of white Plexiglas. The larger one was made of black Plexiglas and was equipped with a removable cover of the same material to allow the compartment to be in darkness. A tensor lamp illuminated the small compartment. The floor of the larger compartment consisted of two oblique stainless steel plates folded at the bottom through which a constant current could be delivered. On the training day each mouse was placed in the lit compartment, facing away from the dark compartment. When the mouse had stepped with all four paws into the dark side, the door was closed, the step-through latency was recorded, and two foot shocks (0.4 mA, 50 Hz, 2 s) were delivered with an interval of 5 s. The maximum initial step-through latency allowed as a criterion for the animals entering the trial was 15 s. The mouse was then removed from the apparatus and returned to its home cage. Retention was tested 0.5 or 24 h later following a similar procedure, except that no shock was administered. A maximum step-through latency of 180 s was allowed in the test session.

For both contextual and cued fear conditioning, mice were trained within the same session, with the following protocol: the pretrial time of 1 min in the conditioning box (the same used for shuttle box) was followed by 15 s tone (conditioned stimulus, 3,000 Hz, 80 dB). During the last 5 s of tone a foot shock of 0.75 mA was delivered and after 15 s the procedure was repeated 5 times. During the training period, acquisition of the freezing response was monitored and no differences were found between the two groups. The freezing response to conditioned stimulus was monitored 0.5 h and 24 h after training for both tests: for contextual conditioning, mice were monitored for freezing for 2 min in the box used for training. For cued conditioning, mice were placed in a new, neutral cage, and freezing was monitored for 1 min in the absence of sound (pre-conditioned stimulus freezing) and for 1 min in the presence of a continuous sound (conditioned stimulus freezing). In both tests freezing was scored every 5 s.

The Morris navigation test was carried out in an open-field water maze of 1.5 m in diameter and filled with opaque water at the temperature of  $25 \pm 1^\circ\text{C}$ , located in a laboratory that contained prominent extra-maze cues. A hidden 15-cm-diameter platform was used. Trials lasted a maximum of 120 s. Spatial training consisted of 18 trials (6 per day) during which the platform was left in the same position. After 3 days of learning, the platform was moved to the opposite position and reversal learning was monitored for 2 additional days (6 trials per day).

For the radial maze test the apparatus was a grey plastic maze with eight identical arms radiating from an octagonal starting platform (perimeter,  $7 \times 8$  cm). On each training trial a 20-mg food pellet was placed at the end of each arm and the animal was placed facing a randomly selected direction on the central platform. Animals received one trial per day; each daily trial terminated

when eight choices were made or 15 min had elapsed. An arm choice was defined as placement of all paws on a maze arm. An error was committed when an animal enters a previously visited arm.

**Electrophysiology.** Slices of amygdala and hippocampus were prepared using standard methods and media. Brains were removed to ice-cold artificial cerebrospinal fluid (ACSF, 119 mM NaCl, 2.5 mM KCl, 1.3 mM MgSO<sub>4</sub>, 1.0 mM NaH<sub>2</sub>PO<sub>4</sub>, 26.2 mM NaHCO<sub>3</sub>, 2.5 mM CaCl<sub>2</sub> and 11 mM glucose), cut on a Vibratome or a gravity tissue chopper at 400  $\mu$ m, and maintained in a submersion-type chamber at 28–32  $^\circ\text{C}$ . Extracellular field potentials were recorded using glass pipettes filled with 1 M NaCl or carbon-fibre electrodes placed in the basolateral amygdala or in stratum radiatum of hippocampal CA1. CA1 responses were evoked by stimulation of the Schaffer collaterals using bipolar or monopolar stainless steel electrodes, and responses in the basolateral amygdala were elicited by stimulation of the lateral amygdala with monopolar stainless steel electrodes.

Received 18 April; accepted 15 August 1997.

- Lowy, D. R. & Willumsen, B. M. Function and regulation of Ras. *Annu. Rev. Biochem.* **62**, 851–891 (1993).
- Martegani, E. *et al.* Cloning by functional complementation of a mouse cDNA encoding a homologue of CDC25, a *Saccharomyces cerevisiae* RAS activator. *EMBO J.* **11**, 2151–2157 (1992).
- Cen, H., Papageorge, A. G., Zippel, R., Lowy, D. R. & Zhang, K. Isolation of multiple mouse cDNAs with coding homology to *Saccharomyces cerevisiae* CDC25: identification of a region related to Bcr, Vav, Dbl and CDC24. *EMBO J.* **11**, 4007–4015 (1992).
- Shou, C., Farnsworth, B. G. N. & Feig, L. A. Molecular cloning of cDNAs encoding a guanine-nucleotide-releasing factor for Ras p21. *Nature* **358**, 351–354 (1992).
- Farnsworth, C. L. *et al.* Calcium activation of Ras mediated by neuronal exchange factor Ras-GRF. *Nature* **376**, 524–526 (1995).
- Mattingly, R. R. & Macara, I. G. Phosphorylation-dependent activation of the Ras-GRF/CDC25<sup>Mm</sup> exchange factor by muscarinic receptors and G-protein  $\beta\gamma$  subunits. *Nature* **382**, 268–272 (1996).
- Finkbeiner, S. & Greenberg, M. E. Ca<sup>2+</sup>-dependent routes to Ras: mechanisms for neuronal survival, differentiation, and plasticity? *Neuron* **16**, 233–236 (1996).
- Marshall, C. in *Guidebook to the Small GTPases* (eds Zerial, M. & Huber, L. A.) 65–73 (Oxford Univ. Press, 1995).
- Pawson, T. Protein modules and signalling networks. *Nature* **373**, 573–580 (1995).
- Rosen, L. B., Ginty, D. D., Weber, M. J. & Greenberg, M. E. Membrane depolarization and calcium influx stimulate MEK and MAP kinase via activation of Ras. *Neuron* **12**, 1207–1221 (1994).
- Zippel, R. *et al.* Ras-GRF, the activator of Ras, is expressed preferentially in mature neurons of the central nervous system. *Mol. Brain Res.* **48**, 140–144 (1997).
- Sturani, E. *et al.* The Ras guanine nucleotide exchange factor is present at the synaptic junction. *Exp. Cell Res.* **235**, 117–123 (1997).
- Plass, C. *et al.* Identification of *Grf1* on mouse chromosome 9 as an imprinted gene by RLGS-M. *Nature Genet.* **14**, 106–109 (1996).
- Celio, M. R. Calbindin D-28k and parvalbumin in the rat nervous system. *Neuroscience* **35**, 375–475 (1990).
- Büeler, H. *et al.* Normal development and behaviour of mice lacking the neuronal cell-surface PrP protein. *Nature* **356**, 577–582 (1992).
- Schutz, R. A. & Izquierdo, I. Effect of brain lesions on rat shuttle behavior in four different tests. *Physiol. Behav.* **23**, 97–105 (1979).
- Cahill, L. & McCaughy, J. L. Amygdaloid complex lesions differentially affect retention of tasks using appetitive and aversive reinforcement. *Behav. Neurosci.* **104**, 532–543 (1990).
- Kim, J. J. & Fanselow, M. S. Modality-specific retrograde amnesia of fear. *Science* **256**, 675–677 (1992).
- Morris, R. G. M. Place navigation impaired in rats with hippocampal lesions. *Nature* **297**, 681–683 (1982).
- Müller, U. *et al.* Behavioral and anatomical deficits in mice homozygous for a modified  $\beta$ -amyloid precursor protein gene. *Cell* **79**, 755–765 (1994).
- Olton, D. S., Walker, J. A. & Gage, F. H. Hippocampal connections and spatial discrimination. *Brain Res.* **139**, 215–308 (1978).
- Martinez, J. L. & Derrick, B. E. Long-term potentiation and learning. *Annu. Rev. Psychol.* **47**, 173–203 (1996).
- Chapman, P. F., Kairiss, E. W., Keenan, C. L. & Brown, T. H. Long-term synaptic potentiation in the amygdala. *Synapse* **6**, 271–278 (1990).
- Zucker, R. S. Short-term synaptic plasticity. *Annu. Rev. Neurosci.* **12**, 13–31 (1989).
- LeDoux, J. E. Emotion: clues from the brain. *Annu. Rev. Psychol.* **46**, 209–235 (1995).
- Maren, S. & Fanselow, M. S. The amygdala and fear conditioning: has the nut been cracked? *Neuron* **16**, 237–240 (1996).
- Chapman, P. F. & Bellavance, L. L. Induction of long-term potentiation in the basolateral amygdala does not depend on NMDA receptor activation. *Synapse* **11**, 310–318 (1992).
- Watanabe, Y., Ikenaya, Y., Saito, H. & Abe, K. Roles of GABA(A), NMDA and muscarinic receptors in induction of long-term potentiation in the medial and lateral amygdala *in vitro*. *Neurosci. Res.* **21**, 317–322 (1995).
- Mayford, M., Abel, T. & Kandel, E. R. Transgenic approaches to cognition. *Curr. Opin. Neurobiol.* **5**, 141–148 (1995).
- Bourchuladze, B. *et al.* Deficient long-term memory in mice with a targeted mutation of the cAMP-responsive element-binding protein. *Cell* **79**, 59–68 (1994).

**Acknowledgements.** We thank F. Casagrande for her help with ES cell work, A. Plücker, K. Brennan and M. Lemaistre for generating germline chimaeras from the second independent ES cell clone, K.-P. Giese and A. Silva for providing their Ras-GRF mouse mutant strain before publication, R. Morris, R. Zippel, E. Martegani, L. Alberghina, A. Oliverio and P. Orban for critically reading the manuscript and F. Peverali for helping with artwork. R.B. was supported by a long-term Human Frontier Science Program Organization (HFSP) postdoctoral fellowship, L.M. by a long-term EMBO fellowship, S.G.N.G. and C.H. by the Wellcome Trust, and A.R. by BBSRC. The work was partially supported by the Italian Association for Cancer Research (AIRC), by Progetto Finalizzato AGRO of the Italian National Research Council (CNR) and by CEE (to E.S.), by the Swiss National Science Foundation (to H.-P.L. and D.P.W.), by HFSP (to H.-P.L. and S.G.N.G.) and by MRC (to P.F.C.).

Correspondence and requests for materials should be addressed to R.K. (e-mail: Klein@EMBL-Heidelberg.de).